Journal of Nuclear Materials 389 (2009) 432–435

Contents lists available at ScienceDirect

Journal of Nuclear Materials

journal homepage: www.elsevier.com/locate/jnucmat

# Modeling the influence of high dose irradiation on the deformation and damage behavior of RAFM steels under low cycle fatigue conditions

J. Aktaa *, C. Petersen

*Forschungszentrum Karlsruhe GmbH, Institute for Materials Research II, Hermann-von-Helmholtz-Platz 1, 76344 Eggenstein-Leopoldshafen, Germany*

ARTICLE INFO

*Article history:*
Received 17 December 2008
Accepted 16 February 2009

ABSTRACT

A viscoplastic deformation damage model developed for RAFM steels in the reference un-irradiated state was modified taking into account the irradiation influence. The modification mainly consisted in adding an irradiation hardening variable with an appropriate evolution equation including irradiation dose driven terms as well as inelastic deformation and thermal recovery terms. With this approach, the majority of the material and temperature dependent model parameters are no longer dependent on the irradiation dose and only few parameters need to be determined by applying the model to RAFM steels in the irradiated state. The modified model was then applied to describe the behavior of EUROFER 97 observed in the post irradiation examinations of the irradiation programs ARBOR 1, ARBOR 2 and SPICE. The application results will be presented and discussed in addition.



## 1. Introduction

Reduced activation ferritic martensitic (RAFM) steels, among others EUROFER 97 and F82H, are promising candidates as structure materials for first wall components of future fusion power plants [1,2]. During an operation period of 2 years, the structure material shall be subjected to an irradiation dose of up to 100 dpa (displacements per atom) yielding remarkable irradiation induced embrittlement and changes in its mechanical behavior [3,4]. Considering these changes correctly in the design assessment procedure of the components is a precondition for a reliable operation. Therefore, constitutive models describing the deformation and damage behavior of RAFM steels in the irradiated state under operation loadings are required.

In our approach, we started developing a deformation damage model describing the behavior of RAFM steels in the un-irradiated state [5]. The model accounts for many characteristics originating from the unique microstructure of these materials, among others the non-linear strengthening behavior under monotonic loading, complex non-saturating softening under cyclic loading and material deterioration under creep-fatigue loading [5]. Within the work reported here, the model was then modified to take irradiation into consideration by modeling the irradiation induced hardening and its interaction with the deformation and damage behavior. The resulting irradiation hardening model comprises the hardening induced by neutron irradiation as well as its alteration due to inelastic deformation and its recovery at high temperatures. All these phenomena are observed in post irradiation examinations on RAFM steels. However, the applicability of the irradiation hardening model developed is not restricted to RAFM steels and it can be extended to other materials showing at least qualitatively similar behavior.

Irradiation induced hardening physically is a result of numerous irradiation damage mechanisms which will be reviewed briefly below. They are the basis of the irradiation hardening model developed which will be illustrated later on. Afterwards application of the model to EUROFER 97 will be presented and discussed.

## 2. Irradiation damage mechanisms

Kinetic energy exchanges between energetic neutrons and atoms or between knocked-on atoms and other atoms in the lattice create both simple lattice defects, such as interstitial atoms and vacancies, and complex defects, such as displacement spikes [6]. Simple lattice defects can combine to form vacancy clusters which might reach a critical size and collapse to form stacking faults bounded by dislocation loops [7]. Displacement spikes consist of void regions containing vacancy clusters and some highly strained regions containing interstitials. In addition to lattice defects originating from atomic displacement neutrons are captured by atomic nuclei which subsequently transmute to new elements and possible co-product, such as helium or other noble gases [8]. Since these gases are highly insoluble in the lattice they interact with vacancies and form gas bubbles.

Vacancy clusters, dislocation loops, displacement spikes and helium gas bubbles can be considered as obstacles of different types which impede dislocation motion, increase strength and reduce ductility. They all can be formed in RAFM steels during neutron irradiation causing the so-called irradiation induced hardening. Hereinafter, they will just be referred to as obstacles of different types.

* Corresponding author. Tel.: +49 7247 824946; fax: +49 7247 824980.
*E-mail address:* aktaa@imf.fzk.de (J. Aktaa).

0022-3115/$ - see front matter © 2009 Elsevier B.V. All rights reserved.
doi:10.1016/j.jnucmat.2009.02.032

## 3. Modeling of irradiation induced hardening

The theory of the cutting of an obstacle by a dislocation line suggest that the resulting hardening $\sigma_H$ should be proportional to the square root of the obstacle's volume density $N$ provided that the mean obstacle diameter remains constant. Since we may have $n_H$ different types of obstacles where each type $i$ has its specific volume density $N_i$ and causes a specific amount of hardening $\sigma_{H,i}$ the overall hardening results in

$$\sigma_H = \sum_{i=1}^{n_H} \sigma_{H,i} \quad \text{with } \sigma_{H,i} = h_i\sqrt{N_i}, \tag{1}$$

$N_i$ is expected to be initially proportional to the neutron dose $\phi$ but as the dose increases a saturation effect may occur which limits the obstacle volume density to $N_{s,i}$ [9]. Accordingly, for the evolution of $N_i$ the following can be written:

$$\dot{N}_i = a_i(N_{s,i} - N_i)\dot{\phi}, \tag{2}$$

$h_i$, $a_i$ and $N_{s,i}$ are temperature and material dependent parameters. While $h_i$ reflects how strong the dislocation pileup by the obstacle type $i$ is, $a_i$ is directly related to the formation rate of this obstacle type with respect to irradiation dose, and $N_{s,i}$ gives the maximum volume density can be obtained for this obstacle type achieving a balance between initiation and annihilation. Hence, these parameters are strongly influenced by the material specific microstructure. Assuming that they are known the irradiation induced hardening and the respective increase of yield stress can be determined using the equations above.

However, inelastic deformation and lattice slip activities, respectively, are expected to resolve irradiation defects at least within the associated slip bands [10], such that the volume density of certain obstacle types decreases while the material deforms inelastically. On the other hand, since irradiation induced defects would restrict largely the number of active slip bands the inelastic deformation can be localized microscopically by the forming of channels. Healing of irradiation induced defects is expected to be limited and to be highest in the channel band. To describe the resulting change in $N_i$ as an average over the volume of the representative volume element – whose behavior is in fact modeled here – the following modification of Eq. (2) is proposed:

$$\dot{N}_i = a_i(N_{s,i} - N_i)\dot{\phi} - b_i(N_i - N_{l,i})\dot{p}, \tag{3}$$

$\dot{p}$ is the uniaxial equivalent inelastic strain rate which can also be interpreted as a volume average for the inelastic deformations possibly localized in channels within the representative volume element. $N_{l,i}$ gives the volume density of the irradiation induced obstacles remaining after a sufficiently large amount of inelastic deformation. Assuming that a sufficiently large amount of inelastic deformation would remove always the same amount of irradiation induced hardening $N_{l,i}$ can be determined as:

$$N_{l,i} = \left\langle \sqrt{\max_{-\infty<\tau<t} N_i(\tau)} - \sqrt{N_{r,i}} \right\rangle^2, \tag{4}$$

$b_i$ and $N_{r,i}$ are additional temperature and material dependent parameters. $b_i$ is directly related to the healing rate of the obstacle type $i$ with respect to inelastic deformation and $N_{r,i}$ represents the amount of this obstacle type which is formed at sufficiently high irradiation dose and can not be resolved by inelastic deformation. The brackets $\langle\,\rangle$ operate as follows on the term in between: $\langle x\rangle = (x + |x|)/2$.

At a sufficiently high temperature diffusion processes may contribute to the healing of irradiation induced defects and, thus, to static recovery of irradiation induced hardening. This can be described by adding a static recovery term in Eq. (3) resulting in

$$\dot{N}_i = a_i(N_{s,i} - N_i)\dot{\phi} - b_i(N_i - N_{l,i})\dot{p} - r_i N_i^{q_i}, \tag{5}$$

with $r_i$ and $q_i$ denoting further temperature and material dependent parameters. Irradiation induced hardening $\sigma_H$, the evolution of which can now be calculated using Eqs. (1) and (5) even under inelastic deformation and high temperature dwell conditions, is assumed to influence the deformation and damage behavior like isotropic hardening by increasing the size of the inelastic yield surface in stress space. Accordingly, the deformation damage model already developed for RAFM steels in the reference un-irradiated state under low cycle fatigue conditions [5] is simply modified to cover irradiation effects by incorporating $\sigma_H$ in the flow rule for inelastic deformation as follows (refer to [5]):

$$\dot{\varepsilon}^{in} = \left\langle \frac{|\Sigma| - \sigma_H - k}{Z} \right\rangle^n \operatorname{sgn}(\Sigma) \qquad \text{with } \Sigma = \frac{\sigma}{\psi(1-D)} - \Omega, \tag{6}$$

$\dot{\varepsilon}^{in}$ and $\sigma$ denote the inelastic strain rate and the applied stress, respectively. $\Omega$, $\psi$ and $D$ are internal state variables describing the kinematic hardening, the isotropic softening and the damage, respectively. $k$, $Z$ and $n$ are temperature and material dependent parameters whereas $k$ is equal to the initial yield stress and, thus, determines the initial size of the inelastic yield surface.

## 4. Application of the model to EUROFER 97

Application of the model is anyhow limited to the data available so far for EUROFER 97 from the literature and ongoing irradiation programs. Hence, the values of the model parameters can be determined at certain temperatures. We started to use the model to describe the increase in yield stress determined after irradiation in post irradiation tensile testing. For this purpose, literature data [11] as well as the data determined recently within the irradiation programs SPICE and ARBOR 1 and 2 were considered. Assuming that hardening is induced by only one type of obstacles ($n_H$ in Eq. (1) is equals 1), the model yields the following dependence of $\sigma_H$ and yield stress increase, respectively, on the irradiation dose $\phi$:

$$\sigma_H = h\sqrt{N_s}(1 - \exp(-a\phi))^{0.5}. \tag{7}$$

Fitting this relation to the experimental values of $\sigma_{H,0.2}$ ($\sigma_H$ at 0.2% inelastic deformation), a fairly good description is obtained with $a = 0.132\ \text{dpa}^{-1}$ and $h\sqrt{N_s} = 523.5$ MPa (see Fig. 1). It should be noticed that the parameters $a$ and $N_s$ depend on the irradiation temperature only, while the parameter $h$ reflects the dependence of $\sigma_H$ on the temperature at which it is determined (test temperature).

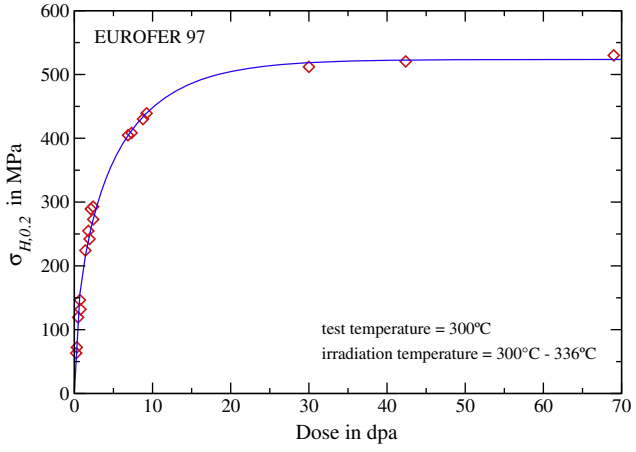


**Fig. 1.** Irradiation-induced hardening as a function of irradiation dose; comparison between experimental data (markers) and model description (solid line).

For the data considered the test temperature (300 °C) is approximately equals the irradiation temperature.

To describe the changes of $\sigma_H$ within the course of inelastic deformation the stress – inelastic strain curves measured in tensile tests on EUROFER 97 irradiated with different doses are compared with the curve obtained for EUROFER 97 in the reference un-irradiated state at the same temperature (300 °C). By subtraction in the small strain range (<5%) the decrease of $\sigma_H$ with increasing inelastic deformation can be determined starting from its initial value after irradiation and 0.2% inelastic deformation $\sigma_{H,0.2}$ (see Fig. 2). For the value of $\sigma_H$ after a certain amount of accumulated inelastic deformation $p$, the following relation can be derived from the model (Eqs. (1) and (5)) by neglecting static recovery:

$$\sigma_H = \left[(\sigma_{H,0.2} - \sigma_r)^2 + (\sigma_{H,0.2}^2 - (\sigma_{H,0.2} - \sigma_r)^2)\exp(-b(p - 0.002))\right]^{0.5}. \quad (8)$$

Also this relation delivers a fairly good description of the experimental data with $b = 78.5$ and $\sigma_r = h\sqrt{N_r} = 298.6$ MPa (see Fig. 2).

Since the temperature of 300 °C is too low particularly for static recovery, the remaining parameters of the model $r$ and $q$ can be assumed to be equal to 0 at this temperature. For higher temperatures, however, these two parameters can be determined best by performing annealing heat treatments on irradiated specimens at the respective temperature with different durations and measuring afterwards the resulting decrease of the yield stress and the irradiation induced hardening, respectively. When applying the model (Eqs. (1) and (5)) the dependence of $\sigma_{H,0.2}$ on the annealing duration $t$ reads

$$\sigma_{H,0.2} = \left[-r^*(1-q)t + (\sigma_{H,0.2}^0)^{2(1-q)}\right]^{0.5/(1-q)}, \quad (9)$$

with $r^* = rh^{2(1-q)}$ and $\sigma_{H,0.2}^0$ being the value of $\sigma_{H,0.2}$ before the annealing heat treatment. Within ARBOR 2 irradiation program such annealing experiments are conducted on EUROFER 97 tensile specimens irradiated with a dose of 69 dpa at 332 °C. The specimens are annealed at 550 °C for 1 and 3 h, respectively, and subsequently tested at 350 °C. From the measured tensile curves the values of $\sigma_{H,0.2}$ are extracted and plotted versus the annealing duration in Fig. 3. Fitting of Eq. (9) to these values results in a fairly good description (see Fig. 3), with $r^* = 5.707 \times 10^{-5}$ MPa$^{2(1-q)}$/sec and $q = 1.288$ representing the values of these parameters at 550 °C.

After determining the parameters of the irradiation induced hardening model for EUROFER 97 at 300 °C, the model is coupled

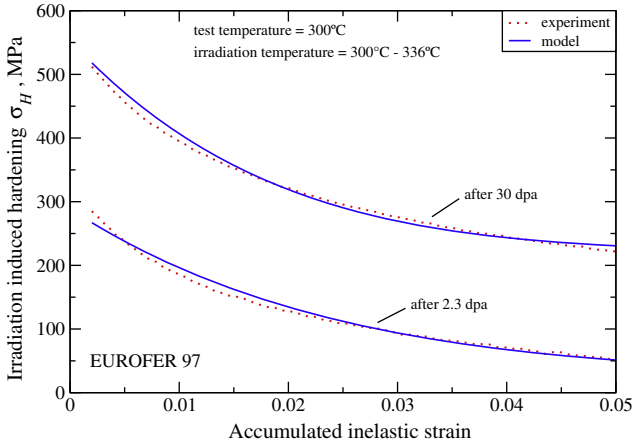


**Fig. 2.** Influence of inelastic deformation on irradiation-induced hardening; comparison between experimental data (doted lines) and model description (solid lines).

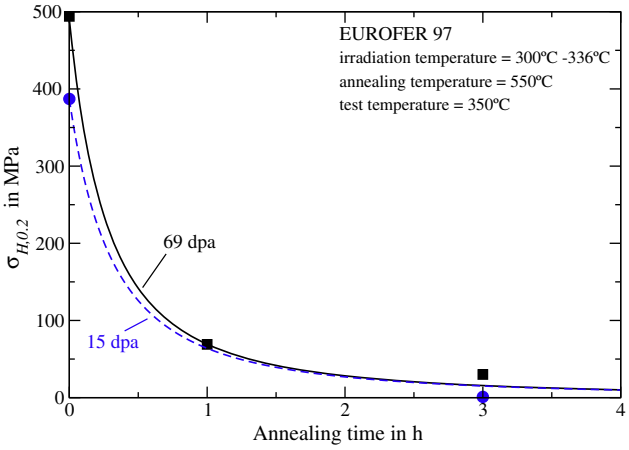


**Fig. 3.** Influence of annealing time on irradiation-induced hardening; comparison between experimental data (makers) and model description (lines).

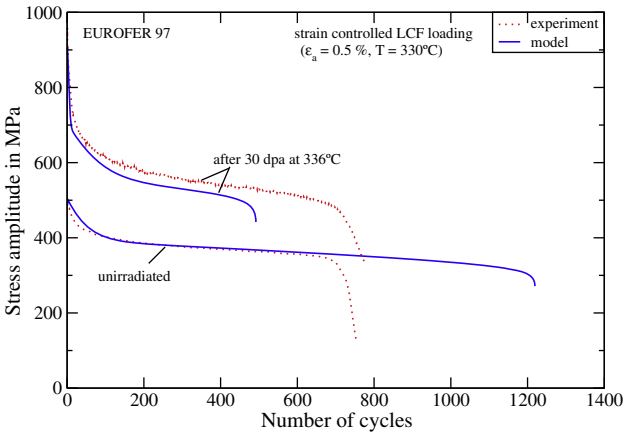


**Fig. 4.** Prediction of the cyclic softening and lifetime behavior of un-irradiated and irradiated EUROFER 97, respectively, in low cycle fatigue tests; comparison between experimental data (doted lines) and model description (solid lines).

with the deformation damage model developed for RAFM steels, as it was described in the previous section, and used for predicting the material behavior of irradiated EUROFER 97 in post irradiation low cycle fatigue (LCF) tests. The tests were performed within the irradiation program ARBOR 1 at 330 °C, which is almost equal to the irradiation temperature. The quality of the prediction is illustrated exemplarily in Fig. 4 by comparing the model prediction with the experimental observations. In this comparison the stress amplitude versus the number of cycles is considered for two LCF tests performed on EUROFER 97 in the un-irradiated and irradiated (30 dpa) state, respectively. As obvious from Fig. 4, the cyclic softening as well as the lifetime are predicted fairly well by the model. For both tests, the pronounced decrease of the stress amplitude particularly in the first cycles is reproduced qualitatively well and the predicted number of cycles to failure deviates from the experimentally observed value by a factor of less than 2 (see Fig. 4).

## 5. Conclusions

The physically based model developed for the description of irradiation induced hardening does not only allow for the determination of hardening due to neutron irradiation, but also of its alteration under inelastic deformation and high temperature dwell conditions. Its coupling with the model describing the deformation

and damage behavior of RAFM steels in the un-irradiated state provides a powerful tool for the prediction of the constitutive behavior of RAFM steels during and after neutron irradiation under low cycle fatigue conditions. When applying the model to EUROFER 97 after neutron irradiation, fairly good results could be obtained determining the model parameters at 300 °C and predicting the deformation and damage behavior. However, more applications of the model are necessary to determine the model parameters for EUROFER 97 at other temperatures as well as the model parameters for other RAFM steels and to verify furthermore its prediction ability.

## Acknowledgment

This work, supported by the European Communities under the contract of Association between EURATOM and Forschungszentrum Karlsruhe, was carried out within the framework of the European Fusion Development Agreement. The views and opinions expressed herein do not necessarily reflect those of the European Commission.

## References

[1] A. Hishinuma, A. Kohyama, R.L. Klueh, D.S. Gelles, W. Dietz, K. Ehrlich, J. Nucl. Mater. 258–263 (1998) 193.
[2] R.L. Klueh, Curr. Opin. Solid State Mater. Sci. 8 (2004) 239.
[3] E. Gaganidze, H.-C. Schneider, B. Dafferner, J. Aktaa, J. Nucl. Mater. 367–370 (2007) 81.
[4] C. Petersen, A. Povstyanko, V. Prokhorov, A. Fedoseev, O. Makarov, B. Dafferner, J. Nucl. Mater. 367–370 (2007) 544.
[5] J. Aktaa, R. Schmitt, Fusion Eng. Des. 81 (2006) 2221.
[6] A.L. Bement, R.G. Hoagland, F.A. Smidt, H. Liebowitz (Eds.), Fracture, vol. III, Academic Press, 1971, pp. 535–587.
[7] J. Marian, B.D. Wirth, R. Schäublin, G.R. Odette, J.M. Perlado, J. Nucl. Mater. 323 (2003) 181.
[8] R.L. Klueh, D.S. Gelles, S. Jitsukawa, A. Kimura, G.R. Odette, B. van der Schaaf, M. Victoria, J. Nucl. Mater. 307–311 (2002) 455.
[9] M.J. Makin, F.J. Minter, Acta Metall. 8 (1960) 691.
[10] B. Mastel, H.E. Kissinger, J.J. Laidler, T.K. Bierlein, J. Appl. Phys. 34 (1963) 3637.
[11] E. Lucon et al., Fusion Eng. Des. 81 (2006) 917.